Anal. Chem. **1996,** *68,* 3808−3814

Flow Injection Based Renewable Electrochemical Sensor System

Michael Mayer and Jaromir Ruzicka*

Department of Chemistry, Box 351700, University of Washington, Seattle, Washington 98195

A novel class of electrochemical sensors is proposed utilizing electrically conducting beads to form a disposable electrode as well as nonconducting beads to form renewable layers of immobilized enzymes. The concept, aimed to prevent fouling, is tested on an amperometric sensor coupled to nonconducting beads with different immobilized oxidases: galactose, lactate, alcohol, or glucose oxidase, the latter two being used to determine alcohol and gluocse, respectively, in samples of beer and wine. Glucose oxidase was also immobilized on conducting glassy carbon particles to explore the performance of a biosensor where both enzyme *and* electrode can be automatically renewed in less than 1 min. The results confirm that the concept of a flow injection renewable electrochemical sensor (FI-RES) is practical. It provides a novel approach to biosensing, to comparing enzyme activity, to studying enzyme immobilization on different supports, and to voltammetry in general.

Fouling of electrode surfaces has been the Achilles' heel of electroanalytical techniques since their introduction to the assay of samples with a complex matrix. It is well recognized that this problem can be fully avoided only through a periodic renewal of the sensing surface.[1] Indeed, the sucess of polarography was due to the use of the dropping mercury electrode, while present methods such as mechanical surface treatment[2] or pulsed amperometry on noble metal electrodes[3−5] are employed. Pulsed amperometry uses oxidative and reductive cleaning cycles to strip accumulated impurities from the electrode surface, while mechanical surface treatment often requires cell disassembly[2] and lacks reproducibility. The design of amperometric biosensors is even more challenging, as it requires a flawless electrode performance and long-term stability of the immobilized biocomponent. Therefore, if an electrode *and* enzyme surface can be automatically renewed in one step, a wide range of presently available biosensing systems become more reliable in practical use. Also, such a flow injection renewable electrochemical sensor (FI-RES) will be universal, since its response to different analytes can be targeted by automatically exchanging the disposable enzyme layer with another immobilized enzyme.

With this goal in mind, we expanded the principles outlined in previous work on flow injection on renewable surfaces (FI-RS[6,7])- and the concept of fiber-optic renewable sensors[8] to amperometric biosensors. The work presented here proceeded in three stages: (1) use of a renewable enzyme layer on a conventional electrode, (2) development of a renewable electrode with conducting particles, and (3) design of a renewable electrode bearing an enzyme layer.

The principle of FI-RS is based on the introduction of a defined volume of bead suspension into a sequential injection (SI) system,[6−8] where the beads are trapped on the sensing surface of a detector. A selective surface modification of the particles undergoes or induces changes while perfused with the analyte zone. These changes are continuously monitored by a suitable detector. The measuring cycle is concluded by discharging the beads from the flow cell. The unique facet of FI-RS is that a fresh sensing layer can be used whenever needed, and since the amount of beads spent is very small (less than 500 μg is needed to "charge" the cell), the method is economical, even if new beads were to be injected for each measurement. The central component of the sequential injection system is the jet ring cell,[6] which was redesigned in this work to accommodate an amperometric sensor (Figure 1). Initially, the cell is filled with a suitable electrolyte. In step A of Figure 1, bead suspension is introduced through the multiposition valve and the particles are trapped in the flow cell, while the carrier stream escapes radially through the narrow circular gap between the electrode plate and the tube. The beads pack regularly, forced by the liquid stream within the jet ring cell (Figure 1B). The height of this multilayered assembly of beads, positioned in contact with each other and with the electrode surface, can be selected as required by choice of the volume of the injected bead suspension. In the third step (C), the analyte zone is injected and transported to the beads, while the product of the enzymatic reaction (hydrogen peroxide in this work) is detected by measuring the oxidation current. Finally D, the outlet gap is opened by lifting the stainless steel tube, and the beads are flushed out to waste. The entire sequence, including flow rates, injected volume, discarding of the beads, and response monitoring, is computer controlled. Nonconducting beads with immobilized galactose oxidase, glucose oxidase, alcohol oxidase, or lactate oxidase were used to form *renewable enzymatic layers* adjacent to the surface of the platinum working electrode. The biosensor system was used to assay ethanol and glucose in various beer and wine samples. Conducting beads forming a three-dimensional flow-through bead electrode, with and without im-

(1) Johnson, D. C.; Weber, S. G.; Bond, A. M.; Wightman, R. M.; Shoop, R. E.; Krull, I. S. *Anal. Chim. Acta* **1986**, *180*, 187−250.
(2) Sawyer, D. T.; Sobkowiak, A.; Roberts, J. L., Jr. *Electrochemistry for Chemists*, 2nd ed.; John Wiley & Sons: New York, 1995; Chapter 5.
(3) Polta, T. Z.; Johnson, D. C. *J. Electroanal. Chem.* **1986**, *209*, 159−69.
(4) Bindra, D. S.; Wilson, G. S. *Anal. Chem.* **1989**, *61*, 2566−70.
(5) Tüdös, A. J.; Johnson, D. C. *Anal. Chem.* **1995**, *67*, 557−60.
(6) Ruzicka, J.; Pollema, C. H.; Scudder, K. M. *Anal. Chem.* **1993**, *65*, 3566−70.
(7) Pollema, C. H.; Ruzicka, J. *Anal. Chem.* **1994**, *66*, 1825−31.
(8) Egorov, O.; Ruzicka, J. *Analyst* **1995**, *120*, 1959−62.

S0003-2700(96)00524-0 CCC: $12.00

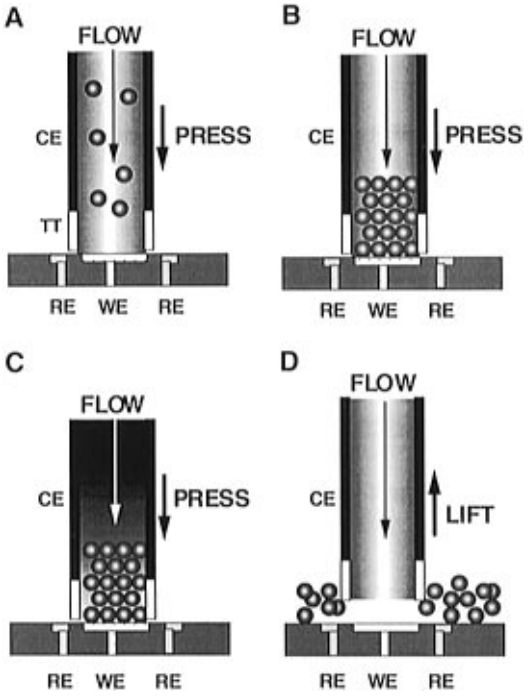

Figure 1. Electrochemical jet ring sensor. (A) Beads are introduced into the cell; (B) beads are trapped and accumulate on the sensor surface; (C) sample (dark shading) is perfused over the beads, and current is continuously monitored; (D) the outlet gap is opened and the beads are discarded. CE, counter electrode, TT, Teflon tube; RE, reference electrode; WE, working electrode.

mobilized glucose oxidase, were used in a model study to explore the concept of *renewable bead electrodes.*

EXPERIMENTAL SECTION

Apparatus. The sequential injection (SI) system was the FIAlab System 3000 (Alitea USA, Seattle, WA) and included the following components: a stepper-motor-driven syringe pump, 3000 steps, syringe volume 1 mL; a six-port selection valve, flow channels 0.8 mm i.d. All Teflon tubing (Upchurch Scientific, Inc., Oak Harbor, WA) had an i.d. of 0.76 mm, and the volume of the holding coil was 900 μL. The amperometric detector utilized a planar concentric platinum electrode system developed in mass production at the "Gesellschaft für Biotechnologische Forschung", GBF mbH, Braunschweig, Germany.[9] The electrodes consist of an aluminum oxide plate (dimensions 2.5 cm × 1.3 cm) with screen-printed Pt layers. The central platinum disk electrode (area 5.5 mm^2) served as the working electrode (Figure 1, WE), on which the beads piled up to form a packed-bed column. The outer ring-shaped Pt electrode (area 28.0 mm^2) served as quasi-reference electrode (Figure 1, RE). The stainless steel tube (0.76 mm i.d., 1.59 mm o.d., Upchurch Scientific, Inc., Oak Harbor, WA) was pressed against the working electrode of the jet ring cell by a spring and served as the counter electrode (Figure 1, CE). A Teflon tube was attached (friction fit) to the tip of the stainless steel tube (Figure 1, TT) to avoid a short circuit between the working and the counter electrode. The potentiostat was a Model 400 EC Detector (EG&G Princeton Applied Research, Princeton, NJ). The stainless steel tubular counter electrode was actuated via computer control by a solenoid (28-C-12V-DC, A420-065452-00, Guardian Electric, Woodstock, IL). Since the prototype flow cell could not be thermostated, care was taken so that ambient temperature was within 20 ± 1 °C.

Materials. The enzymes used in this work, along with the reactions they catalyze, are summarized in Table 1. Controlled pore glass (CPG, mesh size 200−400, mean pore size 697 Å) and oxirane acrylic beads (also called Eupergit C, particle size ~150 μm) were obtained from Sigma (St. Louis, MO). Glassy carbon spherical powder (80−200 μm, type 2) and graphite powder (briquetting grade, −100 mesh, 99.9995%) were purchased from Alfa (Ward Hill, MA). All chemicals were of reagent grade and used without purification.

Buffers. Two different buffers were used: (1) phosphate buffer, prepared by mixing 0.2 M Na_2HPO_4 with 0.2 M NaH_2PO_4 to the desired pH value, and (2) McIlvaine buffer, prepared by mixing 0.1 M citric acid with 0.2 M Na_2HPO_4. Both buffers were degassed for at least 10 min prior to use. Depending on the pH optima of the enzymes in solution, the following phosphate buffers were used for determination of alcohol, pH 7.5; galactose, pH 6.0; and lactate, pH 6.5. For all glucose measurements, McIlvaine buffer, pH 5.9 (pH 5.5 with conducting beads), was used, since the pH optimum of glucose oxidase immobilized on oxirane acrylic beads was found to be between 5.2 and 6.6. The measurements with renewable solid electrodes (without immobilized enzyme) were performed with phosphate buffer, pH 6.8.

Methods. Depending on the mechanical stability of the beads, different methods were applied to maintain homogeneous suspensions. Glassy carbon beads were suspended with a magnetic stirrer; CPG, oxirane acrylic, and graphite powder beads were suspended with a rotating square flask.

The aqueous silanization, activation with glutaraldehyde, and enzyme immobilization on CPG were carried out as described by Weetall.[10] Glucose oxidase (GOx) was coupled by adding 2 mL of 0.05 M phosphate buffer, pH 7.0, containing 200 mg of enzyme to 1.0 g (dry weight) of activated and washed CPG beads. The suspension was stirred gently and allowed to react overnight at room temperature. After extensive washing, the enzyme beads were stored in 40 mL of McIlvaine buffer, pH 5.8, containing 0.1% sodium azide to prevent microbial growth. To remove adsorbed enzyme,[10] the GPG-GOx beads were soaked in 6 M urea (prepared in McIlvaine buffer, pH 5.9) for 45 min and then washed excessively in the same buffer before they were used in the SI system.

The immobilization of alcohol oxidase, galactose oxidase, glucose oxidase, and lactate oxidase on oxirane acrylic beads was carried out as described in the protocol provided by Sigma. The details are summarized in Table 2. For 10 mg of oxirane acrylic beads, 40 μL of enzyme suspension (in phosphate buffer, pH 6.5) was added. After a coupling time of at least 16 h, the beads were washed and suspended in 0.2 M phosphate buffer so that the concentration was at least 2.4 mg (dry weight) of beads per milliliter of suspension.

The immobilization of glucose oxidase on glassy carbon particles was carried out in the following manner:[11] 10 mg of glucose oxidase was dissolved in 1 mL of phosphate buffer, pH 6.8; 10 mg of glutaraldehyde solution (25%) was added; and, after 10 s, 48 mg of glassy carbon particles was added. This mixture

(9) Günther, A.; Bilitewski, U. *Anal. Chim. Acta* **1995**, *300*, 117−25.

(10) Weetall, H. H. *Methods in Enzymology*, Vol. XLIV; Academic Press: New York, 1976; Chapter 10.

(11) Mulchandani, A.; Wang, C.-L.; Weetall, H. H. *Anal. Chem.* **1995**, *67*, 94−100.

Table 1. Enzymes Used in This Work

enzyme[a]	source	catalyzed reaction
alcohol oxidase	*Candida boidinii*	ethanol + O_2 → acetaldehyde + H_2O_2
galactose oxidase	*Dactylium dendroides*	galactose + O_2 → D-*galacto*-hexodialdose + H_2O_2
glucose oxidase[b]	*Aspergillus niger*	β-D-(+)-glucose + O_2 → D-glucono-δ-lactone + H_2O_2
lactate oxidase	*Pediococcus* sp.	L-lactate + O_2 → pyruvate + H_2O_2

[a] All enzymes were purchased from Sigma (St. Louis, MO). [b] Type II.

Table 2. Immobilization of Alcohol, Galactose, Glucose, and Lactate Oxidase on Oxirane Acrylic Beads

enzyme	bead amount (g)	concn of enzyme suspension (mg/mL)	volume of enzyme suspension (mL)	coupling time (h)
alcohol oxidase	0.25	50.0	1.00	37
galactose oxidase	0.04	12.5	0.16	85
glucose oxidase	2.00	37.5	8.00	19
lactate oxidase	0.10	17.5	0.40	61

was allowed to react for 20 h at room temperature. The beads were washed and suspended in phosphate buffer, pH 6.8.

All bead stock suspensions were stored at 4 °C. The bead suspensions used in the sequential injection system were prepared daily from the bead stock suspensions and contained 2.4 mg (dry weight) of beads per milliliter of buffer, except the suspensions used for the glucose measurements with conducting beads and the graphite powder suspensions, which contained 1 mg of beads per milliliter of buffer. The suspensions with glassy carbon beads contained 1 μL of a 1.0 % (v/v) aqueous Triton X-100 solution per milliliter of buffer.

Experimental Protocol. For the measurements with nonconducting beads and graphite powder beads, the sequential injection system was filled with carrier buffer solution, and the potential of the working electrode was set to + 300 mV vs Pt. The measurement cycle comprised the steps listed in Table 3.

The measurements with the glassy carbon electrode (without immobilized enzyme) were done in continuous-flow mode. Therefore, protocol steps 6 and 7 were not performed, and the carrier was pumped continuously at 1.00 mL/min (see Figure 5).

The measurements with the glassy carbon *enzyme* electrode were done with the same protocol as for the nonconducting beads, except that the flow rate during step 5 was 1.00 mL/min and the flow was stopped between 15 and 50 s after the perfusion had begun (see Figures 6 and 7). A potential of +400 mV vs Pt was applied for the measurements with increasing enzyme bead amounts and +300 mV for the calibration graph with the enzyme bead electrode.

Assay of Real Samples. Alcohol and glucose in real samples were determined by standard addition. For the determination of alcohol, the beer samples were diluted 1000−1667-fold with carrier buffer (phosphate buffer, pH 7.5). First, the response of the diluted sample *without* enzyme beads trapped in the jet ring cell was measured (blank signal). Then, the response of the same sample *with* beads was recorded, and finally, the response of the sample with a known added amount of alcohol was measured with enzyme beads in the cell. The blank signal was multiplied by a factor of 0.85 to take into account that the analytical signal would have been 15% lower if acrylic beads (blank beads, without enzyme) would have covered the working electrode. This was necessary because beads on the electrode partly blocked the access of an electroactive compound to the electrode. For the determination of the glucose content, the same beer and wine samples (see Table 5) were diluted 3.3−30 times with carrier buffer (McIlvaine buffer, pH 5.9). The standard addition was carried out in a similar fashion as described for the alcohol measurements.

Reference Methods. The reference method for alcohol in beer and wine was performed using the test kit "Ethanol UV method for the determination of ethanol in foods and other samples" from Boehringer Mannheim (Indianapolis, IN). The measurements were done after the procedure "Simplified determination of ethanol in beer, wine and brandy" which is described in the test kit package. Prior to the analysis, the samples (see Table 5) were diluted 1000-fold with purified water. The reference method for glucose in beer and wine was performed with the "Glucose Trinder, Quantitative enzymatic determination of glucose in serum or plasma at 505 nm" from Sigma. This procedure (No. 315) was provided by Sigma. With both reference methods, standard addition was performed on three beer samples and on the wine sample to check the results of the test.

RESULTS AND DISCUSSION

Renewable Enzyme Layer Using Nonconducting Beads. Increasing volumes of bead suspension (50−800 μL) comprising oxirane acrylic or CPG beads with immobilized glucose oxidase (GOx) were injected (indicated as section A, Figure 3), and the obtained response curves are superimposed in Figure 2. By increasing the height of the bead column, the contact area between enzyme and substrate and the mean residence time in the enzyme reactor increased, resulting in increased hydrogen peroxide production. Thus, the baseline recorded during section B preceded a peak (section C), the height of which was directly proportional ($y = (318/8\ \text{nA mg}^{-1})x + 137.6$ nA; $r = 0.9993$, $N = 15$, y is current, x is bead amount) to the amount of beads (in the range from 0.48 to 5.60 mg of oxirane acrylic-GOx beads) trapped in the jet ring cell (Figure 2, inset). Note that, due to forward flow, the reaction product H_2O_2, produced throughout the length of the enzyme reactor, was transported to the electrode surface. However, during the stopped-flow period (section D), only the hydrogen peroxide produced next to the working electrode contributed to the signal due to diffusion-limited mass transfer. Therefore, once the critical amount of beads was exceeded (>0.12 mg), the analytical signal in the stopped-flow section was independent on the amount of beads trapped in the jet ring cell, as can be seen in Figure 2. When the flow was resumed (section E), a second peak was observed, the height of which was dependent on the length of the bead column but also on the duration of the stopped-flow period. This peak was caused by hydrogen peroxide which accumulated in the enzyme reactor

Table 3. Experimental Protocol

step	event	flow rate (mL/min)
1	aspirate 0.60 mL of carrier buffer	7.50
2	aspirate 0.25 mL of bead suspension into the holding coil and flush it to waste	2.00
3	aspirate a selected volume of bead suspension (0.01−0.40 mL) and transport it to the jet ring cell; settle bead bed with remaining 0.60 mL of carrier buffer	2.00
4	aspirate 0.60 mL of carrier	7.50
5	aspirate 0.10 mL of sample; perfuse over the beads, begin current scan when perfusion begins	0.12−4.00
6	stop flow between 24 and 60 s after perfusion begins	typically 0.50
7	resume flow and perfuse remaining carrier buffer over the beads	1.00
8	aspirate 3.00 mL of carrier buffer, open gap, and flush the spent beads to waste	10.00

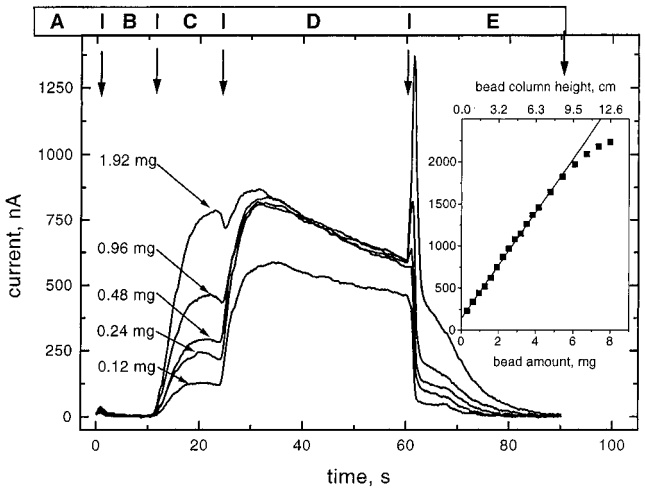

Figure 2. Response curves for increasing amounts of oxirane acrylic-GOx beads trapped in the jet ring cell. Glucose concentration of the sample, 2.00 mM. Measurement protocol: (A) load the jet ring cell with beads before current scanning; (B) baseline current before sample hits the bead layer; (C) perfuse sample (0.50 mL/min) through the beads and over the detector; (D) stopped-flow period; (E) flow is resumed (1.00 mL/min). The inset shows the peak heights during constant flow (C) as a function of the bead amount. The indicated bead amounts refer to the dry weight.

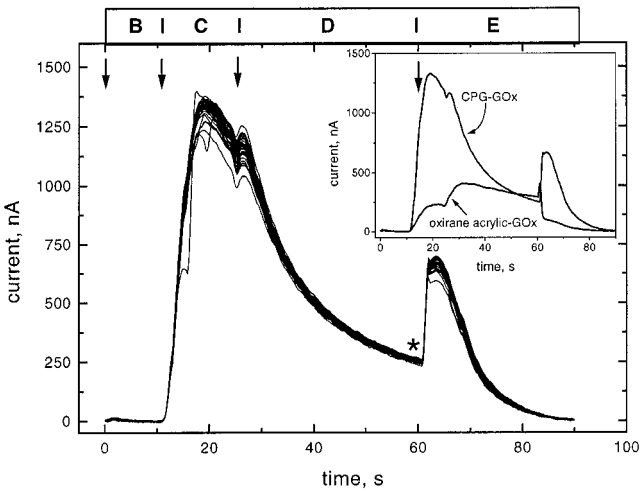

Figure 3. Repeatability of 41 glucose injections with the same CPG-GOx bead layer. Glucose concentration, 1.00 mM. Bead amount, 0.96 mg dry weight. The asterisk indicates where data were collected. See Figure 2 for description of B−E.

Table 4. Regression Statistics for Alcohol, Galactose, Glucose, and Lactate Calibration[a]

analyte	slope (nA/mM)	r	linear range (mM)	detection limit (mM)
alcohol	36.3	0.998	0.17−1.71	0.085
galactose	75.7	0.998	0.01−5.00	0.005
glucose	281.5	0.999	0.01−1.50	0.005
lactate	257.8	0.999	0.005−2.00	0.005

[a] The zero intercept of the calibration curve was within the limits of experimental error.

during the stopped-flow period and was then perfused over the working electrode upon resuming flow.

A similar behavior was found with glucose oxidase immobilized on CPG beads: The response 35 s after the flow was stopped was independent of the bead amount, given that at least 0.048 mg of beads was introduced. As opposed to the data obtained with oxirane beads, the response recorded during the constant flow (section C) was approximately 6 times higher (Figure 3, inset), indicating that the CPG-GOx beads carried higher enzyme activity when the same bead amounts of both support materials were compared.

The repeatability using always the same bead layer was investigated by injecting 400 μL of CPG-GOx bead suspension (0.96 mg of beads, dry weight) and perfusing this column 41 times in sequence with a 1.00 mM glucose standard. The response curves are superimposed in Figure 3. Optimum repeatability was achieved when the analytical signal was taken 35 s after the flow was stopped (asterisk, Figure 3). The relative standard deviations obtained at this point were 1.0% with oxirane acrylic-GOx beads and 2.3% with CPG-GOx beads.

Due to the superior repeatability at the end of the stopped-flow period for most measurements, the data for all calibration graphs were taken from this part of the response curve. By replacing the beads in the jet ring cell with oxirane beads containing immobilized alcohol oxidase, galactose oxidase, or lactate oxidase on their surface, the same experimental setup was used to assay the corresponding analytes. Table 4 summarizes the regression data of the calibration graphs for alcohol, galactose, glucose, and lactate, along with the detection limits. In Figure 4, the response curves of all studied biosensors obtained at a concentration of 0.50 mM of each analyte are shown. The highest response in the constant flow section (section C) was recorded with immobilized lactate oxidase, indicating that the activity on the beads was highest for this enzyme. The observed activities of glucose oxidase, galactose oxidase, and alcohol oxidase immobilized on oxirane beads were lower in this order. The signal heights measured with the lactate and glucose biosensor in the

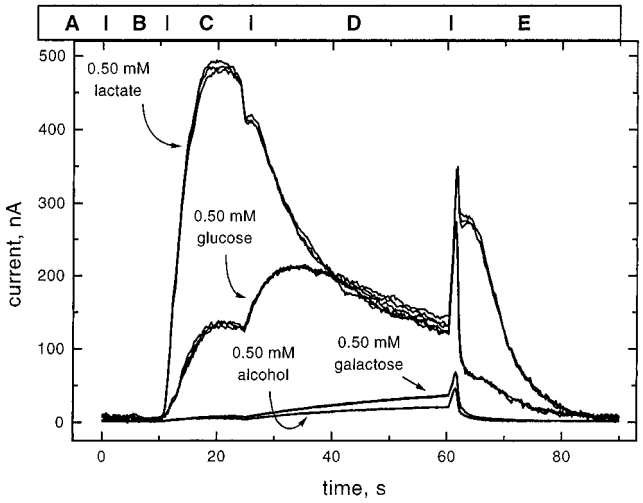

Figure 4. Comparison of the response curves with alcohol, galactose, glucose, and lactate oxidase beads using the same analyte concentration. All four oxidases were immobilized on oxirane acrylic beads. The measurements with each biosensor are shown in triplicate. For description of A−E, see Figure 2.

Table 5. Alcohol and Glucose Determination in Beer and Wine Samples

	alcohol content (% v/v)		glucose content (mM)	
sample	SI method	reference method	SI method	reference method
Rainier Ale	5.0	6.5	20.5	20.0
Pyramid Porter	4.4	5.4	0.5	0.7
Thomas Kemper Amber Lager	4.9	4.2	1.0	0.9
Moosehead Ice	4.8	5.2	0.2	0.4
Brazal Special Amber Lager	5.6	5.3	2.7	2.7
Brazal Bock	7.4	6.0	3.1	3.1
Snoqualmie Chenin Blanc, dry	5.7	8.4	1.2	1.0

stopped-flow section were converging, indicating that the response during stopped-flow was limited by the mass transfer of the analyte rather than by the activity of the immobilized enzymes. This was confirmed by the observation that the long-term stability of all four biosensors was best when the signal was taken at the end of the stopped-flow section.

Measurement reproducibility was also examined by packing a fresh bead column for *each* measurement. The relative standard deviations obtained with 0.96 mg of beads (measured 35 s after the flow was stopped) were 2.9% and 1.1% with oxirane acrylic-GOx and CPG-GOx beads, respectively.

The long-term stability of the renewable glucose biosensor was tested 39 and 60 days after immobilization, during which time the bead stock suspension was kept refrigerated at 4 °C. The responses were found to be 82% and 75% of the original response level. The sensitivity of the galactose biosensor system was 60% of the initial value after 2 months.

The performance of the alcohol and glucose biosensors was tested with beer and wine samples. The results are shown in Table 5 and are in good agreement with the results obtained by the photometric reference methods. A range of beer samples was selected to provide a widest possible variety of matrices: light and dark, "lager" and "bock", clear as well as turbid with suspended matter.

Renewable Electrode Using Conducting Beads. Glassy carbon beads were chosen because the initial experiments

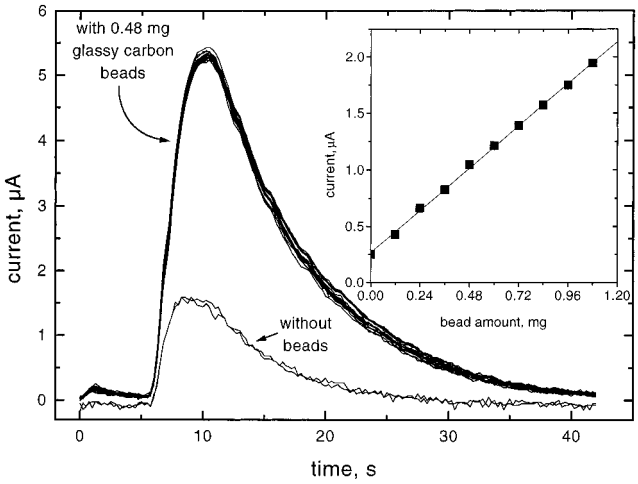

Figure 5. Repeatability of 17 hexacyanoferrate(II) injections obtained with the glassy carbon bead electrode and influence of the bead amount on the sensitivity of the bead electrode. Hexacyanoferrate(II) concentrations, 1.00 mM for the repeatability study and 0.10 mM for the measurements with increasing electrode surface. Applied potential, +130 mV vs Pt.

indicated that they were mechanically robust and relatively easy to keep suspended by stirring. Triton X-100 was added to the bead suspension to limit bead clumping.

Hexacyanoferrate(II) was used to characterize the electrochemical behavior of the bead electrode. At a potential of +700 mV vs Pt, the sensitivity of the bead electrode was approximately 12 times higher than that of the bare platinum working electrode. The current for the oxidation of the hexacyanoferrate(II) standard (concentration 0.10 mM) was still increasing, even at potentials higher than +600 mV vs Pt reference. A possible explanation could be the potential drop in packed-bed electrodes as described by Sioda and Keating.[12]

Operating at a potential of +130 mV, the bead electrode ("charged" with 0.48 mg of glassy carbon beads) yielded a well-reproduced response curve (Figure 5), resolved from the peak current obtained in the absence of beads. The relative standard deviation at the peak maximum was 1.1% (17 perfusions). The inset in Figure 5 shows the current maximum as a function of the electrode surface. Increasing bead amounts (up to 1.08 mg) resulted in increasing peak currents for the oxidation of hexacyanoferrate(II), the current being directly proportional ($y = (1.56\ \mu\text{A mg}^{-1})x + 0.27\ \mu\text{A}$; $N + 10$, y is current, x is bead amount) to the surface area of the bead electrode.[13] The regression coefficient r was 0.9995, indicating excellent reproducibility of the incremental increase of the effective electrode surface. The y-intercept represents the current measured with the bare platinum working electrode. According to Weber and Long,[14] the response of a high-efficiency electrochemical sensor does not proportionally increase with its surface. Therefore, the obtained linear increase of the signal with increasing electrode surface indicated that the bead electrode worked with low efficiency, which was expected since the applied potential of +130 mV was relatively low. The linear increase of the current with increasing bead amount could be used

(12) Sioda, R. E.; Keating, K. B. Flow Electrolysis with Extended-Surface Electrodes. *Electroanalytical Chemistry, a series of advances*, Vol. 12; Marcel Dekker, Inc.: New York and Basel, 1982;
(13) Rieger, P. H. *Electrochemistry*, 2nd ed.; Chapman & Hall, Inc.: New York, 1994; Chapter 6.
(14) Weber, S. G.; Long, J. T. *Anal. Chem.* **1988**, *60*, 903A−13A.

to estimate the mean surface area of the glassy carbon beads. The geometrical area of the Pt working electrode was 5.5 mm^2, corresponding to a current of 0.27 μA (Figure 5). The current obtained with the bead electrode (1.0 mg of beads) was 1.56 μA; therefore, in a rough approximation, the mean surface area of the glassy carbon beads was 32 $mm^2\ mg^{-1}$.

The reproducibility of the response when the bead electrode was packed freshly before each measurement was investigated as a function of the amount of beads introduced. The relative standard deviations were 5.8%, 2.8% and 3.4% with 0.24, 0.48, and 0.72 mg of glassy carbon beads, respectively. In summary, the glassy carbon bead electrode when operated under optimized conditions (+130 mV, 0.48 mg of beads) at continuous-flow exhibited excellent repeatability (RSD 1.1%), showing a linear response for hexacyanoferrate(II) concentrations over almost 6 decades (1.0×10^{-7}–7.5×10^{-3} M; $y = (4275.2\ \mu A\ M^{-1})x - 0.15\ \mu A$, $r = 0.9975$, $N = 12$). The detection limit was 50 nM $[Fe(CN)_6]^{4-}$.

Stopped-flow experiments were carried out with hydrogen peroxide, since this depolarizer is a product of the enzymatic reactions to be investigated later. A potential of +300 mV was applied while a H_2O_2 standard (3.53 mM) was injected. After the current maximum was exceeded, the sample zone was stopped within the bead electrode (1.52 mg of graphite powder beads). The recorded current was inversely proportional to the square root of the time, as predicted by the Cottrell equation.[15] Although the Cottrell equation is derived for planar electrodes and for mass transport-limited conditions,[16] a plot of the recorded current over the inverse square root of the stop time was linear, with a coefficient of correlation $r = 0.9982$.

Renewable Eznyme Electrode. Ideally, both enzyme and electrode surface should be renewable in a single operation. To test this concept, glucose oxidase immobilized on electrically conducting glassy carbon beads was used. Two parameters were investigated to verify the feasibility of the FI-RES concept: the influence of an increasing electrode surface with immobilized enzyme on the response curve and a calibration graph for the target analyte.

By using increasing amounts of conducting enzyme beads in the jet ring cell and by repeated injection of a glucose standard (11.63 mM), a series of response curves was obtained (Figure 6). Interesting differences can be observed when these response curves are compared with those obtained with nonconducting enzyme beads (Figure 2). In section B, the baseline current increased as the amount of conducting beads increased, as expected for an increasing working electrode surface. In section C, when the zone of glucose reached the bead layer, a rise of the current was observed in both systems; however, the response obtained with nonconducting beads was significantly higher. This indicates that the enzyme capacity of the porous polymer beads was higher than that of the graphite beads. Next, in section D, when the flow was stopped, the current steeply increases, yet with conducting beads the slope is determined by the rate of the enzymatic reaction. The current increases continuously and ultimately reaches a steady state (Figure 6), as opposed to the results with nonconducting beads (Figure 2), where the current decreased during the stopped-flow period. The inset in Figure 6 shows the response as recorded at the end of the stopped-flow period as a function of bead amount ($y = (705\ nA\ mg^{-1})x + 49$ nA; $r = 0.9936$, $N = 5$, y is current, x is bead amount). In section E, the flow was resumed, washing hydrogen peroxide from the electrode surface, and finally the beads were discharged. As one would expect, the comparison of Figures 2 and 6 demonstrates the differences in the detection mechanism of these two types of sensors. The use of conducting beads allowed the reaction product to be sensed in situ, and therefore the response curve in the stopped-flow period reflected the kinetics of enzymatic reaction. On the other hand, the nonconducting beads used in the present work seem to accommodate larger amounts of enzyme.

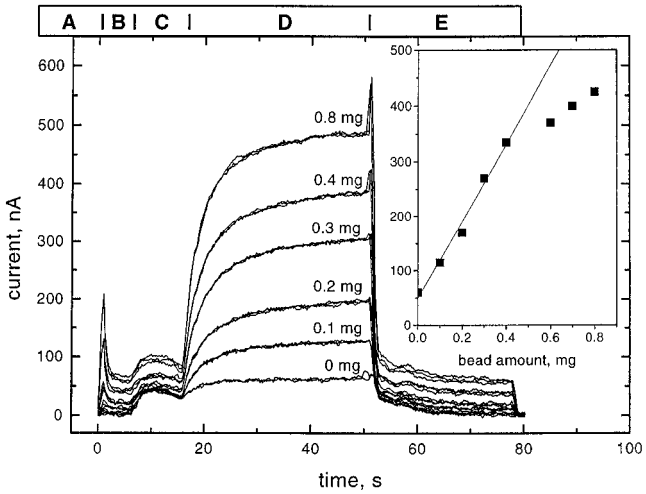

Figure 6. Response curves for increasing amounts of conducting beads bearing glucose oxidase. Glucose concentration of the sample was held constant at 11.63 mM. The indicated bead amounts reflect the dry weight of the glassy carbon beads. Sections A–E refer to the measurement protocol: (A) formation of the enzyme bead electrode by introduction of the beads before the scan begins; (B) baseline current before sample contacts the bead layer; (C) sample is perfused (1.00 mL/min) through the enzyme bead electrode; (D) stopped-flow period; (E) flow is resumed (1.00 mL/min). For each bead amount, three response curves are shown superimposed.

A calibration curve with conducting glucose oxidase beads (0.60 mg of glassy carbon beads) was obtained by injecting glucose standards in the range from 0 mM (carrier buffer) to 11.63 mM (Figure 7). Again, in the stopped-flow section (D), typical first-order reaction rate curves were observed, yielding a calibration curve by measuring either the initial slope or the steady state response. A linear response up to 2.33 mM of glucose ($y = (108.1\ nA\ mM^{-1})x - 1.54$ nA; $r = 0.9997$, $N = 6$) was found when the data were collected at the steady state response.

CONCLUSION

The jet ring cell has been used for the first time in conjunction with an electrochemical detector in a successful attempt to develop a disposable electrode and a renewable biosensor. The experiments with nonconducting enzyme beads have shown that the automated renewal of enzyme bearing surfaces situated close to the amperometric sensor is a feasible and practical approach which allows the biosensor system to be used for a reliable assay of samples with a complex matrix, such as beer or wine. Since the beads are automatically replaced, the sensor system is versatile, as its response can be targeted toward various analytes by simply charging the jet ring electrode with a bead suspension bearing

(15) Rieger, P. H. *Electrochemistry*, 2nd ed.; Chapman & Hall, Inc.: New York, 1994; Chapter 4.

(16) Johnson, D. C.; Ryan, M. D.; Wilson, G. S. *Anal. Chem.* **1986**, *58*, 33R–49R.

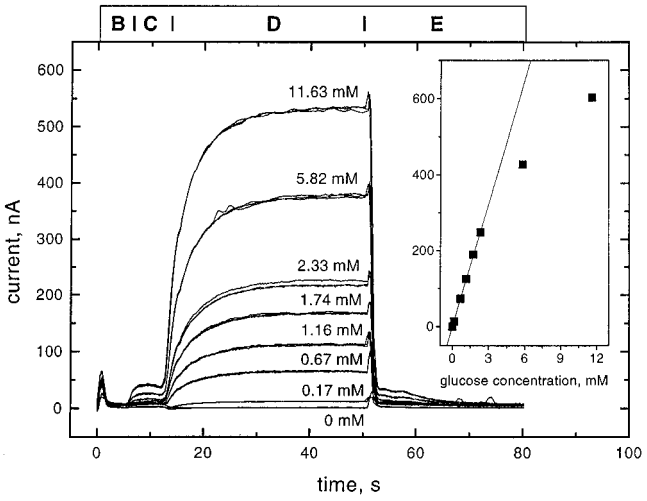

Figure 7. Calibration graph with the glucose oxidase bead electrode. The glucose concentrations are indicated. Enzyme bead amount, 0.60 mg of glassy carbon-GOx beads. Sections B−E, see Figure 6. For each glucose concentration, three response curves are shown superimposed.

the appropriate enzyme. Yet another aspect of the renewability of sensing layers is that the enzyme need not necessarily be convalently bound to the bead surface because it needs only to last for one operational cycle (between 30 s and a few minutes).

Another interesting aspect of the FI-RES technique is its potentially wide measuring range. The sensitivity of the bead electrode can be adjusted through three independent variables: the volume of injected sample, the amount of injected beads, and the length of the stopped-flow period.

In addition to being suited for serial enzymatic assays, the FI-RES technique is a potentially useful tool for automated study of parameters important for engineering and design of packed-bed enzyme reactors. Not only can the efficiency of different enzymes immobilized on the same solid support be compared, as shown in Figure 4, but in a similar manner the efficiency of different immobilization procedures or the suitability of different support materials can be compared with the same experimental setup (Figure 3). Such studies are presently labor intensive, since a large number of miniature columns of different lengths and bead−enzyme combinations must be packed manually and mounted into a flow system, where postcolumn detection is carried out.[17] The opportunity to vary the length of enzyme reactors in an automated and highly repeatable way could be useful to model packed-bed enzyme reactors[18] and to determine characteristic constants such as K_M^{app} and V_{max}^{app} of immobilized enzymes.[17,19]

From the viewpoint of performing enzymatic assays and studying activities of immobilized enzymes, the use of conducting beads is most attractive, as it offers direct insight into the rate of enzymatic reactions, because the reaction product is monitored during its formation in the stopped-flow mode (Figures 6 and 7). The reaction rate measurement offers an additional degree of selectivity, should an unknown interferent produce a noticeable initial current. On the other hand, the nonconducting beads are available in a wide variety of surface functional groups and material properties.

This work is only an initial step, designed to demonstrate the feasibility and practicality of the renewable electrochemical sensor concept. Much more needs to be done in terms of development of a bead electrode with a robust construction and smaller permanent electrode surface (smaller Pt working electrode to establish the electrical contact with the conducting beads) and a more stable Ag/AgCl reference electrode.

On the theoretical side, a study of the mechanism of current transport within the conducting bead layer is needed to provide a better insight into how the bead electrode functions. A large body of literature on packed-bed electrodes[12,20−23] is a useful guide for the optimization of electrode packing and the impact of particle size on rates of depolarizer removal. The role of void volumes, effective area of packed-bed electrodes, and the influence of stopped-flow and continuous-flow regimes on the resulting current needs to be investigated to optimize the FI-RES system. We believe that the conducting bead electrode, operated in FI-RES mode, will not only promote advances in biosensor work but also will lead to novel approaches in the area of preconcentration and detection of traces of compounds that can be preconcentrated on graphite surface *prior* to their voltammetric detection.

ACKNOWLEDGMENT

The authors express their gratitude to G. D. Christian and A. Ivaska for their interest in this work and critical discussion. D. A. Holman assisted in developing the software, and P. J. Baxter helped to edit the manuscript. The “Ernest-Solvay-Stiftung”, the “Gottlieb Daimler-und Karl Benz-Stiftung”, and, to a smaller degree, EPA funded the work of M.M. The screen-printed electrodes were a gift from the biosensor group at the “Gesellschaft für Biotechnologische Forschung”, GBF mbH, Braunschweig, Germany.

Received for review May 29, 1996. Accepted August 7, 1996.[⊗]

AC960524A

[⊗] Abstract published in *Advance ACS Abstracts,* September 15, 1996.

(17) Emnéus, J.; Gorton, L. *Anal. Chim. Acta* **1993**, *276*, 303−18.
(18) Lortie, R.; Pelletier, D. *AIChE J.* **1992**, *38*, 1477−80.
(19) Richter, P.; Ruiz, B. L.; Sánchez-Cabezudo, M.; Mottola, H. A. *Anal. Chem.* **1996**, *68*, 1701−5.
(20) Bisang, J. M. *J. Appl. Electrochem.* **1996**, *26*, 135−42.
(21) Tennakoon, C. L. K.; Bhardwaj, R. C.; Bockris, J. O'M. *J. Appl. Electrochem.* **1996**, *26*, 18−29.
(22) Tamminen, A.; Vuorilehto, K.; Yläsaari, S. *J. Appl. Electrochem.* **1996**, *26*, 113−7.
(23) Bingkun, Y. *J. Appl. Electrochem.* **1990**, *20*, 974−7.